The Astrophysical Journal Letters, 792:L22 (6pp), 2014 September 1 doi:10.1088/2041-8205/792/1/L22

AN ENIGMATIC POINT-LIKE FEATURE WITHIN THE HD 169142 TRANSITIONAL DISK*,†

Beth A. Biller[1,2], Jared Males[3,12], Timothy Rodigas[4], Katie Morzinski[3,12], Laird M. Close[3], Attila Juhász[5], Katherine B. Follette[3], Sylvestre Lacour[6], Myriam Benisty[7], Aurora Sicilia-Aguilar[8,9], Philip M. Hinz[3], Alycia Weinberger[4], Thomas Henning[2], Jörg-Uwe Pott[2], Mickaël Bonnefoy[10,11], and Rainer Köhler[2]
[1] Institute for Astronomy, University of Edinburgh, Blackford Hill, Edinburgh EH9 3HJ, UK; bb@roe.ac.uk
[2] Max-Planck-Institut für Astronomie, Königstuhl 17, D-69117 Heidelberg, Germany
[3] Steward Observatory, University of Arizona, 933 North Cherry Avenue, Tucson, AZ, 85719, USA
[4] Department of Terrestrial Magnetism, Carnegie Institution of Washington, 5241 Broad Branch Road, NW, Washington, DC 20015, USA
[5] Leiden Observatory, Leiden University, P.O. Box 9513, 2300 RA Leiden, The Netherlands
[6] LESIA, CNRS/UMR-8109, Observatoire de Paris, UPMC, Université Paris Diderot, 5 Place Jules Janssen, F-92195 Meudon, France
[7] UJF-Grenoble 1/CNRS-INSU, Institut de Planétologie et d'Astrophysique de Grenoble (IPAG) UMR 5274, F-38041 Grenoble, France
[8] Departamento de Física Teórica, Facultad de Ciencias, Universidad Autónoma de Madrid, E-28049 Cantoblanco, Madrid, Spain
[9] SUPA, School of Physics and Astronomy, University of St Andrews, North Haugh, St Andrews KY16 9SS, UK
[10] Université Grenoble Alpes, IPAG, F-38000 Grenoble, France
[11] CNRS, IPAG, F-38000 Grenoble, France
Received 2014 May 2; accepted 2014 July 14; published 2014 August 20

ABSTRACT

We report the detection of a faint point-like feature possibly related to ongoing planet-formation in the disk of the transition disk star HD 169142. The point-like feature has a $\Delta\mathrm{mag}(L) \sim 6.4$, at a separation of $\sim 0\farcs11$ and position angle $\sim 0^\circ$. Given its lack of an H or K_S counterpart despite its relative brightness, this candidate cannot be explained by purely photospheric emission and must be a disk feature heated by an as yet unknown source. Its extremely red colors make it highly unlikely to be a background object, but future multi-wavelength follow up is necessary for confirmation and characterization of this feature.

Key words: planets and satellites: detection – planets and satellites: formation – planets and satellites: gaseous planets – protoplanetary disks

Online-only material: color figures

1. INTRODUCTION

Transition disks trace a key step in the formation of planetary systems, intermediate between gas-rich protoplanetary disks and debris disks, where primordial gas is cleared away, leaving only remnant dust. These disks are observationally identified by weak mid-IR emission (at $\sim 15\,\mu$m) relative to the Taurus median spectral energy distribution (SED; Najita et al. 2007; i.e., the median SED of primordial disks in the young (<2 Myr) Taurus star-forming region). While numerous physical processes may be responsible for the depletion of gas and dust in transition disks, cleared gaps in particular may be an indicator of a planet or brown dwarf companion in the midst of formation. Thus, these disk systems have been key targets for direct imaging searches for planets.

Transition disks tend to be found in young star-forming regions >100 pc from Earth. Only recently have imaging techniques been available to probe the inner portions of these disks, where planets are likely to form. In the past few years, there have been a number of notable discoveries of companions in transition disks with cleared gaps. Via the interferometric sparse-aperture masking (henceforth SAM) technique (Lacour et al. 2011), Kraus & Ireland (2012) found LkCa 15b, a candidate protoplanet embedded within the disk of a ~2 Myr solar analog. Biller et al. (2012) detected a 0.1–0.4 $M_\odot$ companion in the disk around the Herbig Ae/Be star HD 142527. This binary companion was recently confirmed and shown to be accreting via direct imaging (Close et al. 2014). HD 142527 has a particularly wide gap in its disk (>10–120 AU; Fukagawa et al. 2006; Rameau et al. 2012; Casassus et al. 2012), which may be explained by a stellar companion on an eccentric orbit. Finally, Quanz et al. (2013a) reported an as yet unconfirmed candidate protoplanet detection in the disk of the Herbig Ae/Be star HD 100546.

The Herbig Ae/Be star HD 169142 possesses a nearly face-on transition disk, and has been studied in detail both spectroscopically (Meeus et al. 2001; van Boekel et al. 2005), and through imaging (Habart et al. 2006; Kuhn et al. 2001; Hales et al. 2006; Grady et al. 2007; Fukagawa et al. 2010; Honda et al. 2012; Mariñas et al. 2011). Recently, Quanz et al. (2013b) detected a well-resolved annular gap from 40 to 70 AU via polarized light imaging. Thus, like LkCa 15, HD 142527, and HD 100546, it is an excellent candidate to possess a planetary mass or brown dwarf companion in the midst of formation.

2. STELLAR PARAMETERS

Adopted stellar parameters are presented in Table 1. In general, we adopt the stellar parameters from Table 1 of Quanz et al. (2013b). An accurate age estimate is particularly important for estimating candidate companion properties; HD 169142 has been assigned a fairly wide range of ages. Guimarães et al. (2006) assign a comparatively young age of 1–5 Myr based in HD 169142's H-R diagram position, while Blondel & Djie (2006) claim a similar mass and age as β Pic for HD 169142. Grady et al. (2007) find a comoving companion $9\farcs3$ separated from HD 169142. This object is a 130 mas separation weak-line T Tauri binary, thus they assign an age of 6^{+6}_{-3} Myr for

* Based on observations made with ESO Telescopes at the La Silla Paranal Observatory under program ID 091.C-0572.
† This Letter includes data gathered with the 6.5 Magellan Telescopes located at Las Campanas Observatory (LCO), Chile.
[12] NASA Sagan Fellow.

Table 1
Properties of the HD 169142 System

	Primary	Disk Feature
Distance	145 ± 10[a]	
Age	3–12 Myr[b]	
Proper motion (μ_α, μ_δ)	$(-2.1 \pm 1.5, -40.2 \pm 1.5)$ mas yr^{-1}[c]	
Separation: 2013 July 14 UT	...	$0.11 \pm 0\farcs03$ (∼16 AU)
Position angle: 2013 July 14 UT	...	$0^\circ \pm 14^\circ$
$\Delta L'$	...	6.4 ± 0.3
H (mag)	6.91[d]	...
Ks (mag)	6.41[d]	...
L' (mag)	5.64[e]	12.0 ± 0.3
$M_{L'}$ (mag)	−0.2	6.2 ± 0.3
Spectral type	A7V[f]	...
Estimated mass	1.65 $M_\odot$[f]	...

Notes.
[a] Sylvester et al. (1996), but errors derived here.
[b] Grady et al. (2007).
[c] Høg et al. (2000).
[d] From Two Micron All Sky Survey.
[e] Malfait et al. (1998).
[f] Blondel & Djie (2006).

the entire system. For our analysis here, we thus adopt an age range of 3–12 Myr. Sylvester et al. (1996) derive a photometric distance of 145 pc to HD 169142, based on an A5 spectral type; Blondel & Djie (2006) update this to 151 pc based on a spectral type of A7V. As derived spectral type will strongly affect the photometric distance, we adopt a distance range of 145 ± 10 pc here to account for any uncertainty in spectral typing.

3. OBSERVATIONS AND DATA REDUCTION

3.1. 2013 July VLT NACO Vortex Observations

First epoch observations were conducted using the novel annular groove phase mask (henceforth AGPM) vector vortex coronagraph (Mawet et al. 2013) with the NACO camera at the Very Large Telescope (VLT; Lenzen et al. 2003; Rousset et al. 2003). The AGPM coronagraph uses an AGPM to redirect on-axis starlight out of the pupil (Mawet et al. 2005). In this manner, the AGPM coronagraph enables L' band contrasts of Δmag > 7.5 mag at inner working angles down to $0\farcs09$ (Mawet et al. 2013). HD 169142 was observed in L' from 02:47 UT to 04:54 UT on 2013 July 14, covering nearly an hour both before and after transit. The derotator was turned off to enable angular differential imaging (ADI) techniques. Seeing varied from 1″–2″ over the observation. We used a base exposure time of 0.25 s with 120 coadds and obtained a total of 1 hr 15 minutes on-sky exposure time. Sky frames were interspersed after every 20 frames and 0.05 s unsaturated exposures were taken at the beginning of the sequence. Care was taken to keep the primary star centered under the AGPM. Observation details are presented in Table 2.

Data were flat-fielded and bad-pixel-corrected using dome flats and darks taken as part of ESO standard calibrations. Numerous dust spots are apparent on the AGPM, thus slight misalignments between science and sky frames can produce significant cosmetic errors. Thus, we carefully selected the sky frame that minimized cosmetic errors for each science frame. Out of 126 total science frames, 11 science frames showing significant cosmetic errors even after sky subtraction were discarded. Each frame was centroided on the raw data using the idl routine mpfit2dpeak.

Table 2
Observation Log

Telescope/Instrument	UT Date	Band	Exposure Time	Field Rotation
VLT NACO Vortex	2013 Jul 14	L'	75 minutes	135.2
MagAO CLIO-2 Narrow	2014 Apr 9	H	46 minutes	178.5
MagAO CLIO-2 Narrow	2014 Apr 10	H	30.4 minutes	172.9
MagAO CLIO-2 Narrow	2014 Apr 12	K_S	70 minutes	180.1
MagAO CLIO-2 Narrow	2014 Apr 15	3.9 μm	60 minutes	164.1
MagAO VisAO Narrow	2014 Apr 15	z_p	82.4	176.8

After basic data reduction and centroiding on the center of the coronagraphic mask using the IDL mpfit2dpeak routine, we analyze the data using three independent principal component analysis (PCA) pipelines (following the algorithms of Soummer et al. 2012; Amara & Quanz 2012). All three pipelines yielded similar results—we report here the results using the publically available pipeline of Dimitri Mawet (http://www.sc.eso.org/∼dmawet/DimitriMawet/IDL_PCA_pipeline.html).

3.2. 2014 April Magellan AO Observations

Follow up observations were conducted using the 585 actuator 1000 Hz adaptive secondary adaptive optics (AO) system (MagAO) at the 6.5 m Magellan Clay Telescope (Close et al. 2013). With 378 corrected modes, the MagAO system is one of the highest sampled AO systems on a large telescope (>5 m) and has demonstrated high spatial resolutions (20–30 mas) in the visible (as short as $\lambda = 0.6$ μm; Close et al. 2013). MagAO feeds both a visible (VisAO, 0.5–1 μm) and infrared camera (Clio2, 1–5 μm) simultaneously.

We obtained a total of five data sets for HD 169142 with MagAO from 2014 April 8–15. Observing details are presented in Table 2. Four of these data sets were obtained with the Clio2 Narrow camera, including two H band observations, one K_S band observation, and one 3.9 μm 5% filter observation. We also obtained a deep z' data set using the VisAO camera. The derotator was turned off to enable ADI techniques. All MagAO data was reduced in the standard manner (flat-field correction, sky-subtraction, bad-pixel correction). The H, K_S, and z' data sets remained unsaturated in the core; thus we align our images using the unsaturated core. We then process our data using the independent PCA-based pipelines of CoIs Rodigas and Males (see, e.g., Rodigas et al. 2014; Males et al. 2014). Both pipelines yielded similar results.

At 3.9 μm, we acquired data for HD 169142 as well as for a point-spread function (PSF) star of similar magnitude. We achieved very high Strehl ratios for both stars in dry, photometric conditions. Seeing remained around $0\farcs4$–$0\farcs6$ for the entire night. After image registration, we built a PSF from the nearby star images and subtracted the PSF from each of our MagAO/Clio2 images of HD 169142, then rotated to place north up/east left. Our best subtraction is for a PSF scaling of 115%, which removes the Airy rings quite well. Dark pixels in the core are due to saturation/nonlinearity.

4. RESULTS

In 2013 July, we detected a faint, point-like feature in our L' vortex data set at ∼0° position angle (P.A.), with a separation of $\sim 0\farcs11$. This point-like feature was independently imaged in 2013 June by Reggiani et al. (2014). Multiband follow-upobservations were conducted using Magellan AO in 2014 April. Images from all epochs are presented in Figures 1 and 2. Astrometry and photometry are presented in Table 1. The

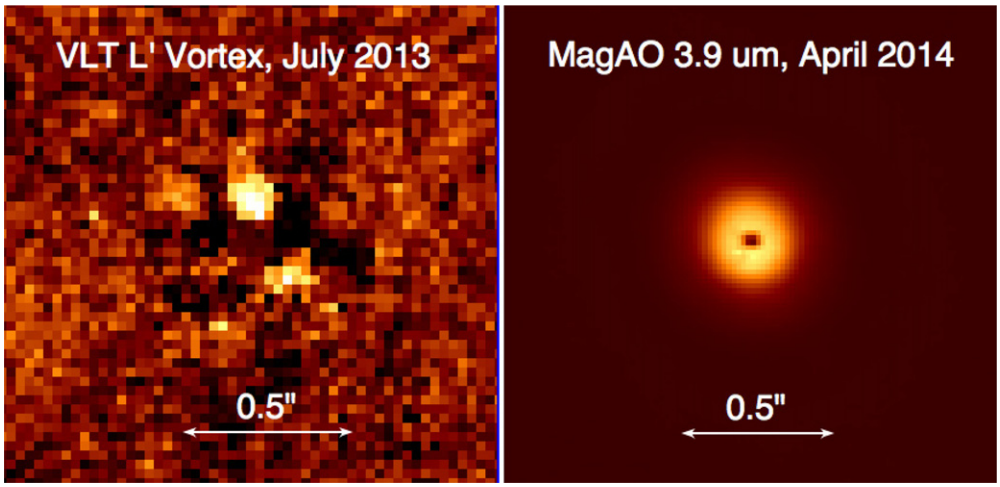

Figure 1. Left: L' 2013 July NACO Vortex image. We find a point-like feature in the disk with $\Delta\mathrm{mag} = 6.4 \pm 0.2$, at a separation of $0\farcs11 \pm 0\farcs03$ and P.A. of $0^\circ \pm 14^\circ$. Right: 3.9 μm 2014 April PSF-subtracted MagAO CLIO-2 image. Dark pixels in the core are due to saturation/nonlinearity. The 2014 April MagAO image reached shallower contrasts than the original vortex image, hence the faint point-like feature is not retrieved. Our non-coronagraphic data set was too shallow to retrieve the candidate ($\Delta\mathrm{mag} = 5.6$ at $0\farcs11$).

(A color version of this figure is available in the online journal.)

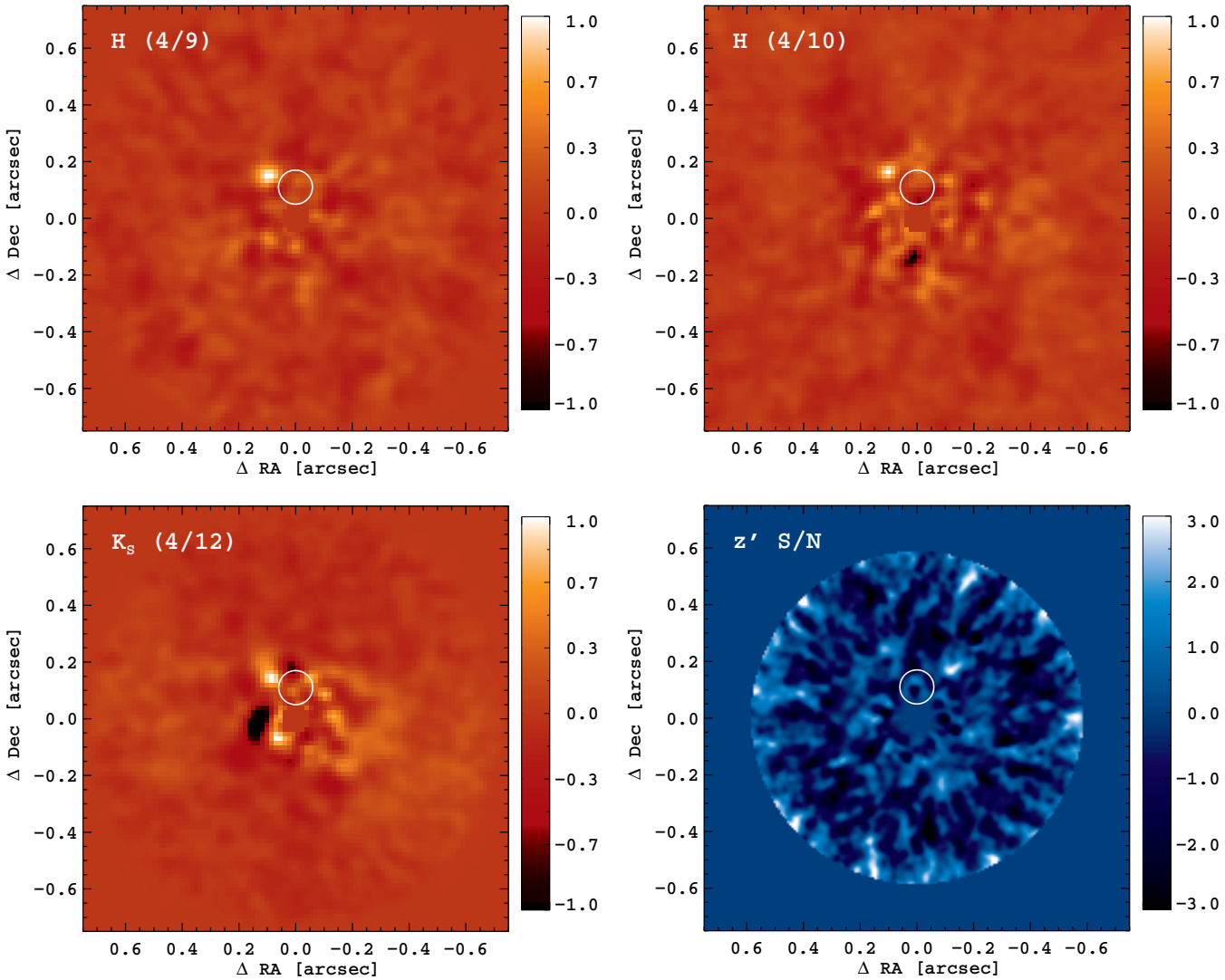

Figure 2. Top left and right: H-band 2014 April MagAO CLIO-2 images over two consecutive nights; bottom left: K-band MagAO CLIO-2 image; bottom right: z'-band 2014 April MagAO VisAO image. All images have been reduced with PCA. The position of the L' point-like feature is circled.

(A color version of this figure is available in the online journal.)

correct rotation to place north up and east left was verified at each epoch. For the 2013 July vortex data, a data set on HD 142527 was acquired on the same run. The bright HD 142527 disk (see, e.g., Fukagawa et al. 2006; Rameau et al. 2012) is correctly derotated by the pipeline. For the 2014 April MagAO data, the correct derotation has been validated using images of the Trapezium cluster.

4.1. 2013 July VLT NACO Vortex Observations

L' photometry and astrometry was derived for the point-like feature by inserting scaled PSF images into the raw data and selecting the fluxes and positions that best match the actual feature. The best astrometry and photometry is presented in Table 1. Assuming a point source, our best subtraction yielded $\Delta\mathrm{mag} = 6.4 \pm 0.2$ for this feature, at a separation of $0\farcs11 \pm 0\farcs03$ and P.A. of $0 \pm 14^\circ$. Given that the inner working angle of the vortex coronagraph is $0\farcs09$ (Mawet et al. 2013), this point-like feature is marginally resolved at best.

To estimate the signal-to-noise ratio (S/N) level of our detection, we calculated the mean and standard deviation in a circular aperture with diameter of λ/D centered on the point-like feature and in the six additional resolution elements available at this separation and then calculated S/N from Equation (9) of Mawet et al. (2014) (appropriate for speckle-dominated regions):

$$\mathrm{S/N} = \frac{\bar{x_1} - \bar{x_2}}{s_2\sqrt{1 + \frac{1}{n_2}}}, \quad (1)$$

where $\bar{x_1}$ is the mean within the aperture containing the feature, $\bar{x_2}$ is the mean of the remaining six resolution elements, s_2 is the standard deviation of the remaining six resolution elements, and n_2 is the number of resolution elements not containing the feature. We find S/N $\sim$ 6 for the detected feature, thus this detection is unlikely to be a false positive—a result which is further bolstered by the independent detection of the same feature by Reggiani et al. (2014).

Initially assuming purely photospheric emission, we estimate mass using Monte Carlo methods to account for the range of possible ages and uncertainties in photometry for this system. An ensemble of 10^6 possible ages are drawn from a uniform distribution running from 3 to 12 Myr. An ensemble of 10^6 absolute magnitudes are simulated, assuming Gaussian errors on photometry and distance (0.3 mag error in Δmag, 10 pc error in distance). We then interpolate with age and single band absolute magnitude to find the best mass for the companion from the DUSTY and COND models of Chabrier et al. (2000) and Baraffe et al. (2002). Mass range histograms are presented in Figure 2. Adopting a 3–12 Myr age range at a distance of 145 pc and the DUSTY models, this candidate would correspond to a relatively high-mass 60–80 M_{Jup} brown dwarf (see Figure 3).

4.2. 2014 April Magellan AO Observations

No counterpart to the L' detection was found in the 2014 April MagAO follow up. Our non-coronagraphic 3.9 μm follow-up imaging was too shallow to retrieve the point-like feature ($\Delta\mathrm{mag} = 5.6$ at $0\farcs11$). However, a 60–80 M_{Jup} object at these ages should have been quite bright in the near-IR (H-band absolute magnitude <7) and have been easily detected given our H and K_S sensitivity. Indeed, our sensitivity is sufficient to detect a $\sim$7–15 M_{Jup} object at this separation and age range. Such a high-mass companion should open up a very wide gap in the disk, inconsistent with the ring at similar radii observed

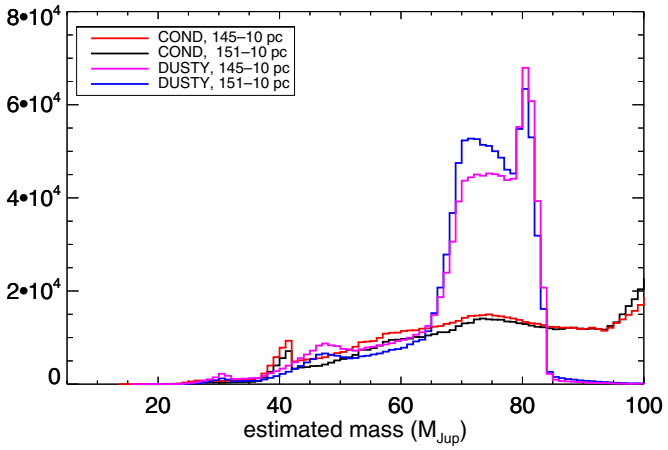

Figure 3. Mass estimate histogram for the point-like feature observed in L'. If due to photospheric emission from a companion, this object would have mass >40 M_{Jup} and an easily detected H and Ks counterpart.
(A color version of this figure is available in the online journal.)

polarimetrically by Quanz et al. (2013b). The lack of a near-IR counterpart to the L' detection signifies that we are not observing the photosphere of a substellar object here but possibly a potential disk feature as its extremely red colors indicate that it is extraordinarily unlikely to be a background object.

We performed radiative transfer calculations to investigate whether or not a passively heated disk "feature" can reproduce the observed point-like source. We used the best fit disk model parameters from Maaskant et al. (2013) to describe an axisymmetric disk. Then, to simulate a clump, we increased the pressure scale height in the disk. The scale height was increased as a two-dimensional Gaussian centered on the observed point source with an FWHM of 7 AU and a peak perturbation of 30%. We used 0.1 μm size astronomical silicates for the dust opacity to get an upper limit on the scattered light perturbations. Larger grains would scatter preferentially forward, perpendicular to the line of sight, which would decrease the contrast between the clump and the central star. Then we measured the contrast on the calculated L' images. We find that a "dust clump" at the position of our candidate would have a contrast of $\sim$17 mag (1×10^{-7}) between the star and the clump, much fainter than the detected candidate.

This result is not surprising, given the distance of the point-like feature from the star. Assuming we observe only thermal dust emission from an irradiated clump, if the clump peaks at L', it would have $T \sim 850$ K. Thus, adopting this as the maximum temperature of a potential dust clump, an irradiated clump with this temperature would be at a distance of the order of 0.6 AU (considering temperature and radius of the primary from Quanz et al. 2013b), inconsistent with the >10 AU separation of this detection. Tentatively, we consider this candidate to be a disk feature heated by an as yet unknown mechanism.

We also marginally detected a candidate companion in H and K_S with a separation of $\sim0\farcs18$ and a P.A. of $\sim33^\circ$, but at low significance (S/N = 3–5, using the same procedure as for the point-like L' feature). These data were taken at two different nods, with very different looking PSFs in the two nods, limiting the precision of our photometry to ±0.5 mag. Thus, while this point source was detected in two different bands on three nights (with S/N $\sim$ 5 in the first data set, but only S/N $\sim$ 3 in the additional data sets), it requires confirmation at an additional epoch, with a more stable PSF, to verify

common proper motion and rule out imaging and reduction artifacts. If real and purely photospheric, this candidate would be a 8–15 $M_{\rm Jup}$ planet/substellar object (DUSTY and COND models). No corresponding L' counterpart was found in the 2013 July L' vortex data set. If purely photospheric, the L' counterpart to this object is expected to have an absolute magnitude >8.5 mag (DUSTY or COND models), corresponding to an apparent magnitude of >14.3 mag. This is considerably below our achieved contrast for this data set at this separation (limiting magnitude of ∼12.7, from insertion and retrieval of PSF images into the raw data). We also do not see a counterpart to this point source in our deep MagAO/VisAO z' data set, down to a contrast of 10^{-4}. If real, the very red colors of this object are inconsistent with background stars with spectral types earlier than mid to late M.

5. DISCUSSION

The known geometry of this disk limits the potential masses of companions associated with imaged asymmetries. Quanz et al. (2013b) image an inner dust ring peaking at 25 AU and an annular gap from 40–70 AU. The L' detection lies within the 25 AU dust ring and may be connected to ongoing companion formation in the disk. If associated with a massive object, it may have had some role in clearing out the region inside this ring. Our tentative H/K detection does not lie within the 40–70 AU gap but is coincident with the 25 AU dust ring. This suggests that any substellar/planetary counterpart to this tentative detection cannot be very massive, as a massive object ($\gtrsim$0.55 $M_{\rm Jup}$) should completely clear away dust from its immediate environment (Kley & Nelson 2012). If massive objects are associated with these detections, they would be some of the closest companions imaged to date. Among confirmed directly imaged exoplanets, only β Pic b, HR 8799d, and HR 8799e have comparably small projected separations (Lagrange et al. 2010; Marois et al. 2008, 2010).

Some disk asymmetries detected via SAM have been described due to forward scattering off an inclined disk (e.g., Cieza et al. 2013; Olofsson et al. 2013). However, HD 169142 is nearly face on (Quanz et al. 2013b), so forward scattering cannot have produced any observable structure in this case.

Our L' detection is also not well described by dust features heated only by the central star; it is simply too far from the star to be heated enough to produce the observed emission. However, bright disk-related features have been observed in other transition disks. For instance, Kraus et al. (2013) detect bright asymmetries via SAM in the H, K', and L' bands within the 15–40 AU inner gap in the pre-transitional disk V1247 Orionis. These asymmetries are not well fit by a companion model; these authors attribute these features to spiral features or accretion streams due to the interaction of the dust disk with the substellar bodies inside the gap responsible for its clearing. Kraus & Ireland (2012) detect a protoplanet candidate (also via SAM) around LkCa 15. While their detection is well fit by a single point source at K, the L detection appears extended and not entirely coincident with the K detection. They interpret the K detection as the protoplanet itself and the L detection as circumplanetary material potentially shocked and heated by jets from the protoplanet.

In the case of HD 169142, the possible energy source for the observed L' disk feature remains unknown. As previously noted, the lack of a H/K counterpart rules out photospheric emission and the L' detection is too strong to be described by passive heating from the star. If due to jets or accretion onto a forming planetary companion, we would expect a Hα counterpart to the L' detection (Close et al. 2014). However, K. B. Follette et al. (in preparation) have observed HD 169142 with MagAO in Hα and do not detect an Hα counterpart to the L' disk feature.

The L' detection may be related to emission line regions inside the HD 169142 disk. Habart et al. (2006) found strong 3.3 μm polycyclic aromatic hydrocarbon (PAH) emission (from a C–H stretching feature of neutral PAHs) in the HD 169142 disk out to 0.″3 (using high-resolution, AO-supported NACO long-slit spectroscopy and along a slit oriented north to south, i.e., intersecting our detection). Maaskant et al. (2014) also find strong PAH emission (however, primarily in ionized features) in the HD 169142 disk, likely stemming from the inner disk gap. A weak blue leak (on the order of 1%) in the NACO L filter might allow us sensitivity to PAH features in the disk. If our L' feature is indeed due to PAH emission, future 3.3 μm follow-up observations should easily retrieve this feature.

6. CONCLUSIONS

We report the detection of a faint point-like structure in the HD 169142 transition disk, also independently detected by Reggiani et al. (2014). This structure has Δmag(L) ∼ 6.4, at a separation of ∼0.″11 and P.A. of ∼0°. Given its lack of an H or K_S counterpart despite its relative brightness, this object cannot be due to the photosphere of a substellar or planetary mass companion and must instead be a disk feature. However, the observed L' detection is too strong to be described by passive heating from the star and ongoing accretion is ruled out by the MagAO Hα non-detection of K. B. Follette et al. (in preparation). While the location of the L' point-like feature right within the disk gap strongly suggests it may be connected to ongoing planet-formation (i.e., whatever process cleared out the gap), the energy source fueling this feature without producing a corresponding near-IR counterpart still remains mysterious. We hope that future multi-wavelength follow-up observations will elucidate the source of this feature—and perhaps in the process refine our understanding of ongoing planet-formation in this disk.

MagAO was constructed with NSF MRI, TSIP, and ATI awards.

REFERENCES

Amara, A., & Quanz, S. P. 2012, MNRAS, 427, 948
Baraffe, I., Chabrier, G., Allard, F., & Hauschildt, P. H. 2002, A&A, 382, 563
Biller, B., Lacour, S., Juhász, A., et al. 2012, ApJL, 753, L38
Blondel, P. F. C., & Djie, H. R. E. T. A. 2006, A&A, 456, 1045
Casassus, S., Perez, M. S., Jordán, A., et al. 2012, ApJL, 754, L31
Chabrier, G., Baraffe, I., Allard, F., & Hauschildt, P. 2000, ApJ, 542, 464
Cieza, L. A., Lacour, S., Schreiber, M. R., et al. 2013, ApJL, 762, L12
Close, L. M., Follette, K. B., Males, J. R., et al. 2014, ApJL, 781, L30
Close, L. M., Males, J. R., Morzinski, K., et al. 2013, ApJ, 774, 94
Fukagawa, M., Tamura, M., Itoh, Y., et al. 2006, ApJL, 636, L153
Fukagawa, M., Tamura, M., Itoh, Y., et al. 2010, PASJ, 62, 347
Grady, C. A., Schneider, G., Hamaguchi, K., et al. 2007, ApJ, 665, 1391
Guimarães, M. M., Alencar, S. H. P., Corradi, W. J. B., & Vieira, S. L. A. 2006, A&A, 457, 581
Habart, E., Natta, A., Testi, L., & Carbillet, M. 2006, A&A, 449, 1067
Hales, A. S., Gledhill, T. M., Barlow, M. J., & Lowe, K. T. E. 2006, MNRAS, 365, 1348
Høg, E., Fabricius, C., Makarov, V. V., et al. 2000, A&A, 357, 367
Honda, M., Maaskant, K., Okamoto, Y. K., et al. 2012, ApJ, 752, 143
Kley, W., & Nelson, R. P. 2012, ARA&A, 50, 211
Kraus, A. L., & Ireland, M. J. 2012, ApJ, 745, 5
Kraus, S., Ireland, M. J., Sitko, M. L., et al. 2013, ApJ, 768, 80
Kuhn, J. R., Potter, D., & Parise, B. 2001, ApJL, 553, L189

Lacour, S., Tuthill, P., Amico, P., et al. 2011, A&A, 532, A72
Lagrange, A.-M., Bonnefoy, M., Chauvin, G., et al. 2010, Sci, 329, 57
Lenzen, R., Hartung, M., Brandner, W., et al. 2003, Proc. SPIE, 4841, 944
Maaskant, K. M., Honda, M., Waters, L. B. F. M., et al. 2013, A&A, 555, A64
Maaskant, K. M., Min, M., Waters, L. B. F. M., & Tielens, A. G. G. M. 2014, A&A, 563, A78
Males, J. R., Close, L. M., Morzinski, K. M., et al. 2014, ApJ, 786, 32
Malfait, K., Bogaert, E., & Waelkens, C. 1998, A&A, 331, 211
Mariñas, N., Telesco, C. M., Fisher, R. S., & Packham, C. 2011, ApJ, 737, 57
Marois, C., Macintosh, B., Barman, T., et al. 2008, Sci, 322, 1348
Marois, C., Zuckerman, B., Konopacky, Q. M., Macintosh, B., & Barman, T. 2010, Natur, 468, 1080
Mawet, D., Absil, O., Delacroix, C., et al. 2013, A&A, 552, L13
Mawet, D., Milli, J., Wahhaj, Z., et al. 2014, ApJ, in press (arXiv:1407.2247)
Mawet, D., Riaud, P., Absil, O., & Surdej, J. 2005, ApJ, 633, 1191
Meeus, G., Waters, L. B. F. M., Bouwman, J., et al. 2001, A&A, 365, 476
Najita, J. R., Strom, S. E., & Muzerolle, J. 2007, MNRAS, 378, 369
Olofsson, J., Benisty, M., Le Bouquin, J.-B., et al. 2013, A&A, 552, A4
Rameau, J., Chauvin, G., Lagrange, A.-M., et al. 2012, A&A, 546, A24
Reggiani, M., Quanz, S. P., Meyer, M. R., et al. 2014, ApJL, 792, L23
Rodigas, T. J., Debes, J. H., Hinz, P. M., et al. 2014, ApJ, 783, 21
Rousset, G., Lacombe, F., Puget, P., et al. 2003, Proc. SPIE, 4839, 140
Quanz, S. P., Amara, A., Meyer, M. R., et al. 2013a, ApJL, 766, L1
Quanz, S. P., Avenhaus, H., Buenzli, E., et al. 2013b, ApJL, 766, L2
Soummer, R., Pueyo, L., & Larkin, J. 2012, ApJL, 755, L28
Sylvester, R. J., Skinner, C. J., Barlow, M. J., & Mannings, V. 1996, MNRAS, 279, 915
van Boekel, R., Min, M., Waters, L. B. F. M., et al. 2005, A&A, 437, 189